A NUCLEAR MAGNETIC RESONANCE SPECTROSCOPY STUDY OF THE SOLVENT DEPENDENCE OF THE BARRIER TO ROTATION IN N,N,N',N'-TETRAMETHYLTHIODICARBONIC DIAMIDE

A thesis presented in partial fulfilment of the
requirements for the degree of
Master of Science in Chemistry
at
Massey University

Lesley Marion Hughes

1977

ABSTRACT

Barriers to rotation were determined from variable-temperature nuclear magnetic resonance spectra. The computer program used to calculate the rotational rates was validated by obtaining results in good agreement with the literature values from studies carried out on neat N,N-dimethylcarbamic chloride. The barrier to rotation for N,N,N',N'-tetramethylthiodicarbonic diamide was measured in a variety of solvents and large variations in activation energy were observed (more than 40 kJ mol^{-1}). The free energies could be correlated with the dielectric constant, the dipole moment, the Hildebrand solubility parameter and the empirical polarity parameters E_T and Z. A linear plot of $\Delta H^{\neq}_{298}$ versus $\Delta S^{\neq}_{298}$ for different solvents was obtained.

Attempts to obtain other systems suitable for NMR study are reported.

ACKNOWLEDGEMENTS

I wish to thank my supervisors Dr. P.D. Buckley and Dr. K.W. Jolley for their help and advice during the study herein summarised. I also wish to thank Alan R. Furness for encouragement and advice and Mrs. J.R. Parry for typing this thesis and thus greatly easing its preparation.

TABLE OF CONTENTS

	Page
Abstract	ii
Acknowledgements	iii
Table of Contents	iv
List of Tables	viii
List of Figures	x
List of Symbols	xii
SECTION ONE	
INTRODUCTION	1
1.1 Description of Nuclear Magnetic Resonance	1
1.1.1 Angular Momentum	1
1.1.2 The Resonance Frequency	1
1.1.3 Chemical Shifts	2
1.1.4 Internuclear Coupling	3
1.1.5 Exchange-induced Variations in Spectra	3
1.2 Quantitative Approach to NMR	4
1.2.1 Classical Derivation of the Bloch Equations	4
1.2.2 Lineshapes and Saturation	7
1.2.3 Exchange between Two Sites and the Absorption Lineshape	9
1.2.4 Use of the Rate Constant	11
1.2.5 Thermodynamic Parameters for Amide Systems	13
SECTION TWO	
INSTRUMENTAL AND EXPERIMENTAL PROCEDURES	17
2.1 The NMR High Resolution Spectrometer	17
2.1.1 Internal Lock and the Spectrometer	17
2.1.2 The Frequency Counter	19

Page

2.2 Variable Temperature Measurements 20

2.2.1 Control of Probe Temperature 20

2.2.2 Temperature Gradients 20

2.2.3 Methods of Temperature Measurement 23

2.3 Preparative Procedures 24

2.3.1 The Glove Box 24

2.3.2 The Cleansing of Glassware 24

2.3.3 Sample Preparation 25

2.3.4 The Freeze Thaw Technique for Sealing NMR Tubes 25

2.3.5 Sample Spectra 25

2.3.6 Digitizing a Spectrum 26

2.4 The Computer Program 26

2.4.1 The Equation on which the Program is Based 26

2.4.2 The Best Fit Parameters 28

2.4.3 Varying τ' so the Value of τ' Converges to a Limit 28

SECTION THREE

NMR STUDY OF THE SOLVENT DEPENDENCE OF THE BARRIER TO ROTATION IN N,N,N',N'-TETRAMETHYLTHIODICARBONIC DIAMIDE 31

3.1 Introduction 31

3.2 The Choice of Solvents 31

3.2.1 Possible Salt Effects 35

3.2.2 Sample Preparation 36

3.3 Data Collection 37

3.3.1 General Problems and Procedures 37

3.3.2 Slow Exchange Spectra 38

3.3.3 Medium Exchange Rate Spectra 40

3.3.4 Low Temperature TTD Spectra in Acetone 40

Page

3.3.5 Low Temperature TTD Spectra in Acetonitrile 42

3.3.6 Low Temperature TTD Spectra in Chloroform 42

3.3.7 Low Temperature TTD Spectra in Dimethyl Sulphoxide-Water 45

3.3.8 Low Temperature TTD Spectra in Pyridine 45

3.3.9 Low Temperature Spectra for TTD in Toluene 50

3.4 Analysis of Spectra 50

3.4.1 Introduction 50

3.4.2 Variation of $\Delta\nu$ 52

3.4.3 Variation in T_2' 56

3.5 Results 56

3.6 Discussion 66

3.6.1 Changes in Spectra and Solutions 66

3.6.2 Errors in Temperature Measurement 67

3.6.3 Changes in $\Delta\nu$ and T_2' 67

3.6.4 Comparison with Previous Results 70

3.6.5 Solvent Effect Studies 71

3.6.6 Studies of TTD in Selected Solvents 74

SECTION FOUR

THE PRELIMINARY INVESTIGATIONS INTO ROTAMERIC SYSTEMS 81

4.1 Introduction 81

4.2 Preparation of Compounds 81

4.2.1 Preparation of 1 H(4-nitrobenzoyl)-pyrrole 81

4.2.2 Preparation of Dimethyl-4-nitrosophenol 81

4.2.3 Preparation of N-Benzyl-N-methoxy-N methylamine 82

4.2.4 Purification of N,N-Dimethylcarbonic Chloride 84

4.3 Description Variable Temperature Spectra for Rotameric Systems 84

Page

4.3.1 3-Methyl-1-(4-methylphenyl)-triazene 84

4.3.2 1-Acylpyrroles 85

4.3.3 4-Acetylpyridine 86

4.3.4 Dimethyl-4-nitrosophenols 87

4.3.5 N,N-Dimethylcarbamic Chloride 89

Appendix A Computer Program LMH 94

Appendix B Spectra of TTD in Acetonitrile and Pyridine 95

Appendix C An Alternative Plot from which to Determine the Thermodynamic Parameters 96

Bibliography 99

LIST OF TABLES

Table		Page
1.1	N,N-Dimethylacetamide in Various Solvents	14
1.2	Salt Effects on Rotational Barriers in N,N-Dimethylacetamide	16
2.1	Temperature Gradients in the NMR Probe	22
2.2	Van Geet's Equations	24
3.1	Substituent Effects on the Rotational Barrier in N,N-Dimethylamides	32
3.2	Solubility of N,N,N',N'-Tetramethylthiodicarbonic Diamide	33
3.3	Concentration of TTD in Each Solvent	36
3.4	Data used to Determine the Low Temperature Parameters in Acetone	41
3.5	Data used to Determine the Low Temperature Parameters in Acetonitrile	43
3.6	Data used to Determine the Low Temperature Parameters in Chloroform	44
3.7	Data used to Determine the Low Temperature Parameters in DMSO-D_2O	46
3.8	Data used to Determine the Low Temperature Parameters in DMSO-D_2O with $NaClO_4$	47
3.9	The Low Temperature Parameters for DMSO-D_2O Solutions	48
3.10	Data used to Determine the Low Temperature Parameters in Pyridine	49
3.11	Data used to Determine the Low Temperature Parameters in Toluene	51
3.12	Analyses of Acetonitrile Data at Various Temperatures	55
3.13	Variation of T_2' for TTD in Chloroform	57
3.14	Slow Exchange Parameters	58

Table		Page
3.15	Kinetic Data for TTD in Acetone	59
3.16	Kinetic Data for TTD in Acetonitrile	60
3.17	Kinetic Data for TTD in Chloroform	61
3.18	Kinetic Data for TTD in DMSO-Water	61
3.19	Kinetic Data for TTD in DMSO-Water and $NaClO_4$	63
3.20	Kinetic Data for TTD in Pyridine	64
3.21	Kinetic Data for TTD in Toluene	65
3.22	Kinetic Data for TTD in Chloroform when T_2' is Varied	68
3.23	Thermodynamic Parameters for TTD in Chloroform at Various Values for T_2'	69
3.24	Comparison of Results for TTD in Chloroform	70
3.25	Solvent Effect Studies	72,73
3.26	Comparison of the Two Acetone and Two DMSO-Water Solutions	75
3.27	Thermodynamic Parameters of N,N,N',N'-Tetramethylthiodicarbonic Diamide in Selected Solvents	76
3.28	Correlations between $\Delta G^{\neq}_{298}$ for TTD in Selected Solvents and Solvent Parameters	78
3.29	Free Energy Changes for Rotation in N,N-Dimethylacetamide and Solvent Parameters	80
4.1	Low Temperature Parameters for DCC	90
4.2	Kinetic Parameters for N,N-Dimethylcarbamic Chloride	91
4.3	Thermodynamic Parameters for the Barrier to Rotation in N,N-Dimethylcarbamic Chloride	92
C-1	Kinetic Parameters for TTD in Chloroform	97
C-2	Thermodynamic Parameters for TTD in Chloroform	98

LIST OF FIGURES

Figure		Following Page
1.1	Energy Levels for $I = \frac{1}{2}$	1
1.2	A Single Dipole Precessing about $\underline{B}_o$	4
1.3	A Random Collection of Precessing Nuclei	4
1.4	The Oscillating Magnetic Field	5
1.5	The Torque on a Dipole in a Field $\underline{B}_1$	5
2.1	The TMS Lock Signal	17
2.2	Difference in Potential Difference between the Two Thermocouples at Different Positions in the Probe	22
2.3	Potential Difference between the Two Thermocouples Versus the Potential of the Probe Thermocouple	22
2.4	Potential Difference between Two Thermocouples Versus the Probe Thermocouple at Varying Ambient Temperature and 30 gm cm^{-3} Pressure	22
2.5	Flow Diagram 1	28
2.6	Best-fit Value of τ'	30
2.7	Flow Diagram 2	30
3.1	Temperature Dependence of $\Delta\omega$ for TTD in Acetonitrile	43
3.2	Temperature Dependence of $\Delta\omega$ for TTD in Pyridine	49
3.3	Residuals Versus Rate Constant at 294 K for TTD in Chloroform	53
3.4	Changes in k with Temperature and Methods of Computer Analysis for TTD in Acetonitrile	55
3.5	$Log_{10}k$ Versus T^{-1} for TTD in Acetone	59
3.6	$Log_{10}k$ Versus T^{-1} for TTD in Acetonitrile	60
3.7	$Log_{10}k$ Versus T^{-1} for TTD in Chloroform	61
3.8	$Log_{10}k$ Versus T^{-1} for TTD in DMSO-d_6-D_2O	62
3.9	$Log_{10}k$ Versus T^{-1} for TTD in DMSO-d_6-D_2O + $NaClO_4$	63

Figure		Following Page
3.10	$Log_{10}k$ Versus T^{-1} for TTD in Pyridine	64
3.11	$Log_{10}k$ Versus T^{-1} for TTD in Toluene	65
3.12	$H^{\neq}_{298}$ Versus $S^{\neq}_{298}$	77
4.1	3-Methyl-1-(4-methylphenyl)-triazene in Acetone-d_6 at 30°C	85
4.2	1H(4-nitrobenzoyl)-pyrrole in Acetone-d_6 at -40°C	86
4.3	1H(4-nitrobenzoyl)-pyrrole in Acetone-d_6 at -84°C	86
4.4	4-Acetylpyridine at 27°C	87
4.5	2,6-Dimethyl-4-nitrosophenol in Acetone-d_6 at -15°C	88
4.6	N,N-Dimethylcarbamic Chloride at 6°C	89
4.7	N,N-Dimethylcarbamic Chloride at 57°C	89
4.8	$Log_{10}k$ Versus T^{-1} for DCC	91
B-1	TTD in Acetonitrile-d_3 at -14°C, -4°C and -1°C	95
B-2	TTD in Acetonitrile-d_3 at 34°C and 50°C	95
B-3	TTD in Pyridine-d_5 at -33°C and 27°C	95
B-4	TTD in Pyridine-d_5 at 37°C and 42°C	95
B-5	TTD in Pyridine-d_5 at 54°C	95

LIST OF SYMBOLS

A,B	Sites which are not equivalent
$\underline{B},\underline{B}_o$	Constant magnetic fields
B_o	Magnitude of $\underline{B}_o$ along the z-axis
$\underline{B}_1$	Oscillating magnetic field
B_x,B_y,B_z	Components of $\underline{B}$ along the x, y, z axes
G	Complex magnetization
G_T	Defined as $\sum_n G_n$
G_n	Magnetization at site n
h	Plancks constant
$\hbar$	$h/2\pi$
I	Spin quantum number
$\underline{i},\underline{j},\underline{k}$	Unit vectors along the x, y, z axes
i	$\sqrt{-1}$
$\mathcal{I}m(G)$	The imaginary part of G
J_{nm}	The coupling constant between groups n and m
k_B	Boltzmann constant
k_n	Defined as $1/\tau_n$
$\underline{M}$	Magnetization of a collection of nuclei
M_o	The component of $\underline{M}_o$ along the z-axis
$M_x\ M_y\ M_z$	The components of $\underline{M}$ along the x, y, z axes
M_{zn}	M_z at site n
m_I	Momentum quantum number
m_{I-x}	A value of m_I
N_n	The number of nuclei at the nth energy level
$\underline{P}$	Angular momentum
P_z	The component of $\underline{P}$ along the z-axis
p_n	The mole fractional population at site n
T	Absolute temperature
T_1	Longitudinal relaxation time

T_2	Transverse relaxation time
T_{2n}	T_2 at site n
U	Energy
u,v	Components of $\underline{M}$ along x', y'
x', y'	Axes perpendicular to the z-axis and rotation at $-\omega$ rad s^{-1}
α	$1/T_2 + i(\omega_o - \omega)$
γ	Magnetogyric ratio
δ	$10^6 (\nu_i - \nu_{TMS})/\nu_{TMS}$; Hildebrand solubility parameter
ε	Dielectric constant
η	Viscosity
θ	Angle between $\underline{B}_o$ and $\underline{\mu}$
$\underline{\mu}$	Magnetic moment of a nucleus
μ_z	z component of $\underline{\mu}$
ν	Frequency of radiation in Hz
ν_o	Operating frequency of the spectrometer
ν_n	Resonance frequency of the nuclei at position n
ν_{obs}	Observed resonance frequency for a time-averaged peak
ν_{TMS}	Resonance frequency for TMS
σ_n	Shielding constant for the nth group of nuclei
σ_{TMS}	Shielding constant for TMS
$\underline{\tau}$	Torque
τ	Defined as $p_A \tau_B$ or $p_B \tau_A$
ω	Angular frequency in rad s^{-1}
ω_o	Defined as $\gamma B_o = 2\pi \nu_o$
ω_1	Defined as γB_1

SECTION 1

INTRODUCTION

1.1 DESCRIPTION OF NUCLEAR MAGNETIC RESONANCE

The first attempts to observe nuclear magnetic resonance (NMR) were made in 1942[1] but it was not until 1946 that resonance signals were actually seen[2,3]. Once the equipment used had become more sophisticated the theory behind the observed phenomena could be elaborated[4,5,6,7,8].

1.1.1 Angular Momentum

Amongst the properties of some isotopes is that of spin which is associated with angular momentum, $\underline{P}$. Angular momentum is a vector quantity with magnitude, $(h/2\pi)\sqrt{I(I+1)}$, and with a component in the z direction given by the expression

$$P_z = m_I \, h/2\pi \qquad 1\text{-}1$$

where I is the spin quantum number which may have values 0, $\frac{1}{2}$, 1, $\frac{3}{2}$, 2 ... and m_I can have values I, I-1, ... 0, ... -(I - 1), - I. Each isotope has a fixed value of I; for the proton, $I = \frac{1}{2}$.

1.1.2 The Resonance Frequency

Nuclei are charged and a spinning charge has an associated magnetic moment, $\underline{\mu}$, related to the angular momentum by the equation

$$\underline{\mu} = \gamma \underline{P}$$

where γ is called the magnetogyric ratio. In a constant uniform magnetic field, $\underline{B}_o$, aligned along the + z direction, the possible orientations of $\underline{\mu}$ (and hence of $\underline{P}$) become non-degenerate (Fig. 1-1) with energies given by

$$U = - \underline{\mu} \cdot \underline{B}_o = - \mu_z B_o \qquad 1\text{-}2$$

where μ_z is the component of $\underline{\mu}$ along the z axis and B_o is the magnitude

Figure 1-1:

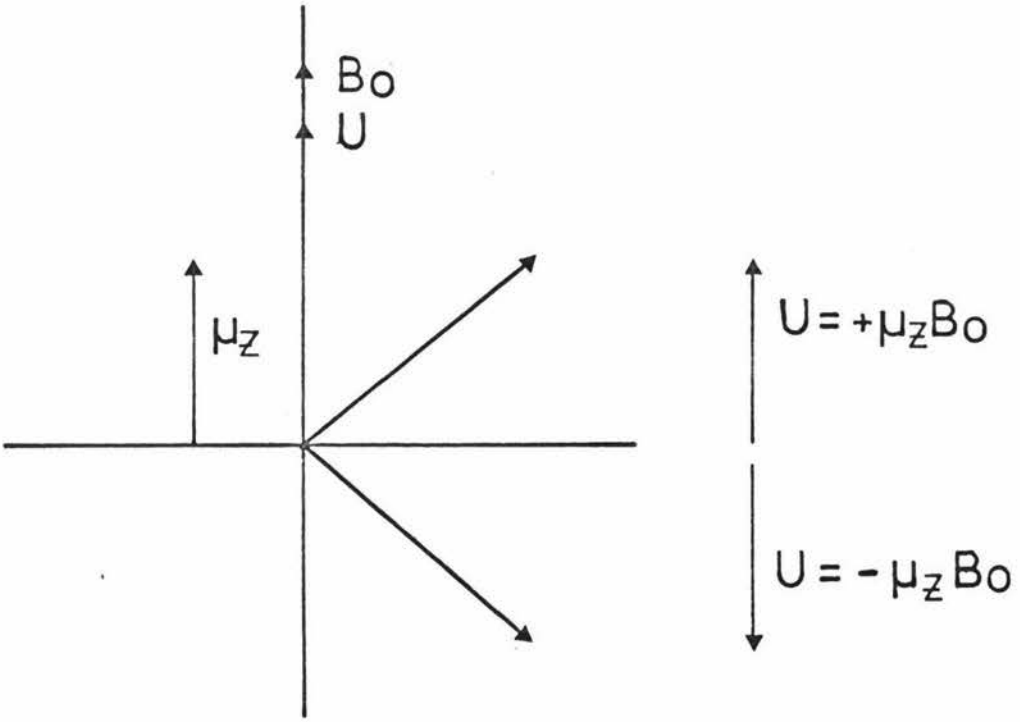

For $I = \frac{1}{2}$, there are two possible orientations of μ with an energy difference

$$\Delta U = 2 \mu_z B_o = \gamma \hbar B_o$$

of $\underline{B}_o$.

Since, for an isotope with even atomic and mass numbers, I = 0, this nucleus does not have spin and is unaffected by the applied magnetic field, it cannot be detected in the nuclear magnetic resonance experiment. Such nuclei include ^{12}C, ^{16}O, ^{28}Si and ^{32}S.

The energy difference, ΔU, between the nth and mth orientations in the magnetic field is

$$\Delta U = U_n - U_m = - (\mu_{zn} - \mu_{zm}) B_o$$

but $\mu_z = \gamma h m_I$

so $U = |\gamma h B_o \Delta m_I|$

where $\Delta m_I = m_n - m_m$

Only transitions between m_n and either m_{n-1} or m_{n+1} are allowed so

$$\Delta m_I = \pm 1$$

and if ν is the frequency of the radiation for such a transition then

$$\Delta U = h\nu = |\gamma h B_o| \qquad 1\text{-}3$$

or

$$\nu = |\gamma/2\pi| B_o \qquad 1\text{-}4$$

1.1.3 Chemical Shifts

If the magnetic environment of a nucleus is not exactly B_o, the applied field, then the frequency which induces resonance will not be $\nu_o = \left|\frac{\gamma}{2\pi}\right| B_o$ but $\nu = \nu_o \pm \Delta$. Such a variation in the local field of a nucleus occurs when neighbouring electrons shield the nucleus from the applied field B_o. Since the electronic environment differs for each group of similar nuclei it is found that for example the resonance signal of a methyl group (CH_3-) is at a different position from that of a methylene group (-CH_2-). This variation is usually expressed as

$$\nu_j = |\gamma/2\pi| B_o (1 - \sigma_j)$$

where σ_j is the shielding constant for the jth group of nuclei.

Since the separation of resonance signals varies with the strength of B_o, the absorption peaks are usually expressed in parts per million (ppm) as $\sigma_j = {}^{\nu_j}/_{\nu_o}$ where ν_o is the operating frequency of the

spectrometer. Unfortunately ν_0 cannot usually be measured accurately because of difficulty in measuring B_0 so often a standard sample is selected and ν_j is measured in ppm from the standard signal. The usual standard in proton NMR is tetramethyl silane (TMS) which contains a single environment for all its protons and resonates at high field from most other proton signals. The values in ppm referenced to TMS are said to be on the δ scale and are defined as

$$\delta = 10^6 \, (\nu_j - \nu_{TMS})/\nu_{TMS} \text{ at constant } B_0 \qquad 1\text{-}5$$

or $$\delta \simeq 10^6 \, (\delta_{TMS} - \delta_j)$$

1.1.4 Internuclear Coupling

The electronic environment, and hence the shielding of the proton, is affected not only by the nature of the group of which it is a part but by neighbouring groups. If the neighbouring group has n protons and as each proton has two possible orientations in the applied magnetic field, the number of possible combinations of spins is n + 1. In the simplest case (referred to as a first order spectrum) the proton may experience a magnetic field due to any one of these combinations and so, for the whole sample, the total absorption peak is split into n + 1 lines with equal separation. The relative intensities of the lines are given by the binomial coefficients (as found in Pascal's triangle).

This interaction is known as spin-spin coupling. Its magnitude is determined by a spin-spin coupling constant (simply referred to as a coupling constant) written as J_{nm} for interaction between spins n and m.

This type of spectral analysis can only be used if $\Delta\nu_{nm} \gg J_{nm}$; in any other case a full quantum mechanical analysis is required to determine chemical shifts and coupling constants.

1.1.5 Exchange-induced Variations in Spectra

Once multiple peaks for a group had been observed[7,8], it was found that the expected splitting in absorption signals was not always apparent.[9]

The lack of coupling was explained by postulating that fast exchange was occurring between several non-equivalent sites so the exchanging nuclei were decoupled from their neighbours whose resonance signals were therefore unsplit.

In most cases the rate of exchange was so fast that only a time-averaged peak was seen at a position ν_{obs} which can be related to the peak positions ν_A and ν_B of the separate sites A and B thus:

$$\nu_{obs} = p_A \nu_A + (1 - p_A)\nu_B = \nu_B + p_A(\nu_B - \nu_A) \qquad 1\text{-}6$$

where p_A is the mole fraction of nuclei at site A.

In some cases at room temperature the peaks at positions ν_A and ν_B are apparent but for intermediate rates of exchange between the two sites the spectrum changes in a regular manner from the slow exchange spectrum with peaks at ν_A and ν_B (for lower temperatures) to the time-averaged peak at ν_{obs} for higher temperatures[10].

1.2 QUANTITATIVE APPROACH TO NMR

The first step in quantitatively describing the observed temperature dependence of the NMR spectrum was to develop a set of equations which would fit the line-shape for a temperature-independent spectrum. These equations were developed, for a simple system, from classical physics but are consistent with quantum mechanical descriptions.

1.2.1 Classical Derivation of the Bloch Equations

If a spinning particle has a magnetic moment $\underline{\mu}$ then, in a uniform external magnetic field $\underline{B}$, a torque $\underline{\tau}$ is exerted on the particle, tending to align $\underline{\mu}$ with $\underline{B}$.

$$\underline{\tau} = \underline{\mu} \wedge \underline{B}$$

Such a torque, combined with the spin, results in the precession of $\underline{\mu}$ about $\underline{B}$ (Fig. 1-2) which can be analysed in terms of angular momentum $\underline{P}$:

Figure 1-2 :

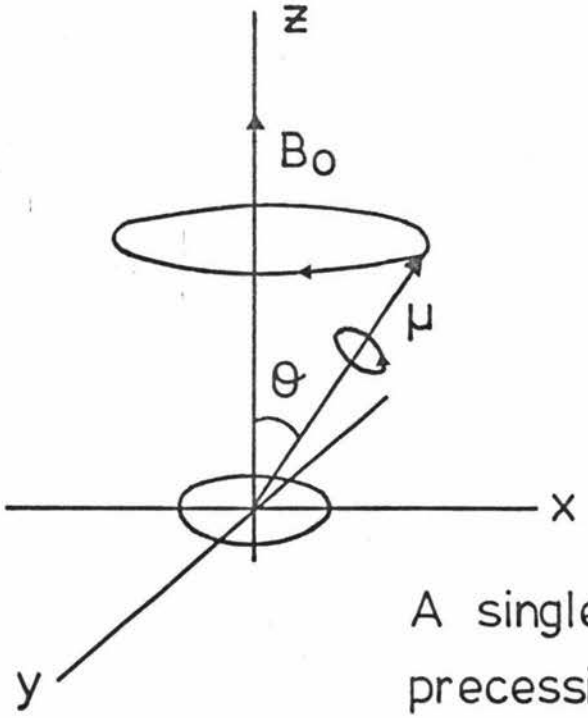

A single dipole precessing about B_o

Figure 1-3:

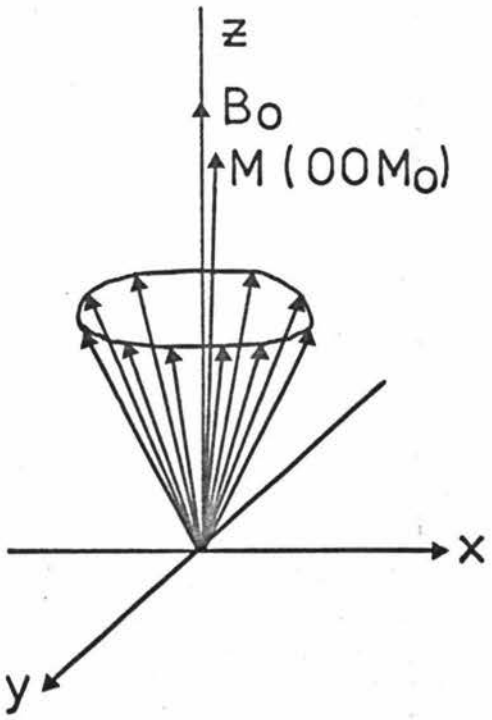

A random collection of nuclei precessing about an external magnetic field B_o along the +z axis

$$\frac{d}{dt}\underline{P} = \underline{\tau} = \underline{\mu} \wedge \underline{B}$$

But $$\underline{\mu} = \gamma \underline{P}$$

So $$\frac{d}{dt}\underline{\mu} = \gamma \frac{d}{dt}\underline{P} = \gamma (\underline{\mu} \wedge \underline{B}) = -\gamma (\underline{B} \wedge \underline{\mu})$$

Since ω_o, the angular velocity of precession, is given by

$$\frac{d}{dt}\underline{P} = \underline{P}\,\omega_o$$

$$\underline{\mu}\,\omega_o = -\gamma (\underline{B} \wedge \mu)$$

or $$\omega_o = |\gamma B|$$

Since $\omega_o = 2\pi\,\nu_o$ this becomes

$$\nu_o = |\gamma/2\pi|\ B$$

This equation was developed from a quantum mechanical basis earlier (see equation 1-4).

In a random collection of nuclei precessing at the same angle, each nucleus has a different phase so that the total magnetic moment (or magnetisation) of the collection, $\underline{M}$, has only a component in the z direction when the collection is in a constant magnetic field $\underline{B}_o$ aligned along the z direction (Fig. 1-3). If the external field varies then $\underline{M}$ will also have components in the xy plane. In the usual continuous wave NMR experiment an oscillating field, 2B, cos t, is applied along the x-axis. Such a field can be regarded as being the sum of two fields, ($B_1 \cos\omega t$, $-B_1 \sin\omega t$, 0) and $B_1 \cos\omega t$, $B_1 \sin\omega t$, 0), counter-rotating about the z axis in the xy plane (Fig. 1-4). Only one of these fields is rotating in the same direction as the precessing moments so only this field ($B_1 \cos\omega t$, $-B_1 \sin\omega t$, 0) can affect the magnetisation $\underline{M}$. The frequency of the applied field, ω , must be that of the precessing moments or the torsional effects at $\omega_o - \omega$ will cancel out those effects at $180 + \omega_o - \omega$ (Fig. 1-5).

The general equations for $\underline{M}$ are

$$\underline{M} = M_x\,\underline{i} + M_y\,\underline{j} + M_z\,\underline{k} \qquad 1\text{-}7a$$

$$\frac{d}{dt}\underline{M} = \left(\frac{d}{dt}M_x\right)\underline{i} + \left(\frac{d}{dt}M_y\right)\underline{j} + \left(\frac{d}{dt}M_z\right)\underline{k} \qquad 1\text{-}7b$$

Figure 1-4:

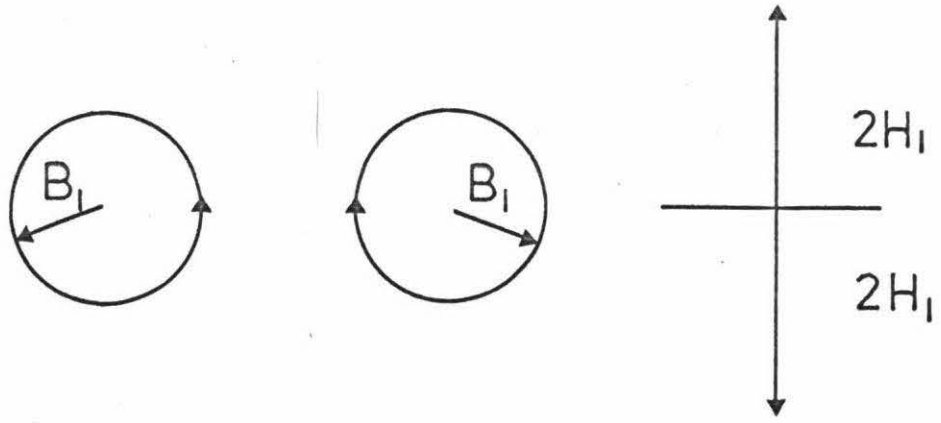

The oscillating magnetic field separated into rotational components

Figure 1-5:

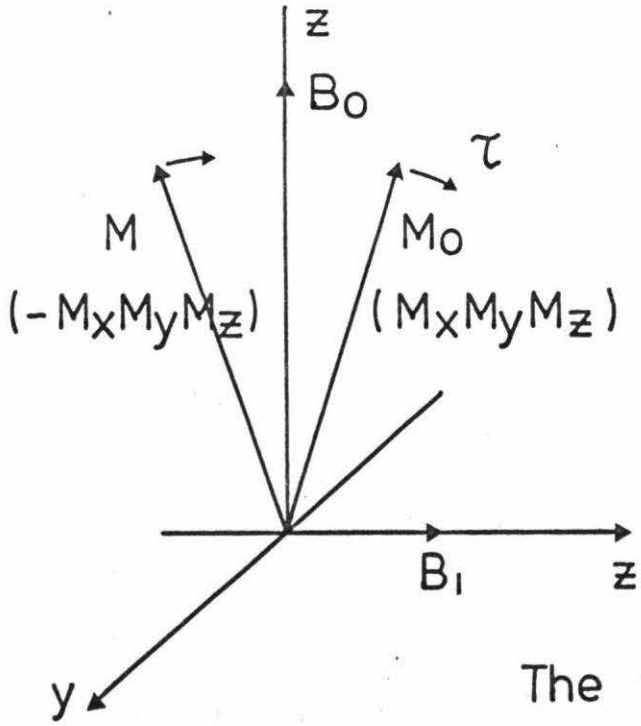

The torque exerted on a dipole by a magnetic field B_1 along the +x axis

If the oscillating field $2B_1 \cos \omega t$ is suddenly switched off then the components (M_x, M_y, M_z) of $\underline{M}$, which are non-zero in the field $\underline{B}$ ($B_1 \cos \omega t$, $-B_1 \sin \omega t$, B_o) will revert to the equilibrium values found in the field $\underline{B}$ ($0,0,B_o$) which were earlier given as $\underline{M}(0, 0, M_o)$. The time constants which govern the exponential decay of M_x, M_y and M_z to their equilibrium values are known as relaxation times. The time constants for the decay of M_x and M_y are assumed to be the same and are called the transverse relaxation time or the spin-spin relaxation time (since the interactions between nuclear spins can relax M_x and M_y without transferring energy to the lattice) and are given the symbol T_2. The time constant for M_z is called the longitudinal relaxation time (since M_z is parallel to the constant field B_o) or the spin-lattice relaxation time (since the energy flow associated with relaxation of M_z is from the nuclear spin system to the lattice) and given the symbol T_1.

The equations governing relaxation are:

$$\frac{d}{dt} M_x = - M_x/T_2 \qquad 1\text{-}8a$$

$$\frac{d}{dt} M_y = - M_y/T_2 \qquad 1\text{-}8b$$

$$\frac{d}{dt} M_z = - (M_z - M_o)/T_1 \qquad 1\text{-}8c$$

Since $\underline{M}$ is the resultant of the collection of magnetic moments it must obey the same type of equation for variation with time as $\underline{\mu}$. Hence

$$\frac{d}{dt} \underline{M} = - \gamma (\underline{B} \wedge \underline{M})$$

$$= - \begin{vmatrix} B_x & M_x & \underline{i} \\ B_y & M_y & \underline{j} \\ B_z & M_z & \underline{k} \end{vmatrix}$$

$$= - \gamma (B_y M_z - B_z M_y) \underline{i} - \gamma (-B_x M_z - B_z M_x) \underline{j} - \gamma (B_x M_y - B_y M_x) \underline{k}$$

When both the oscillating field in the xy plane and the constant field in the z direction are applied

$$\underline{B} = (B_1 \cos \omega t, - B_1 \sin \omega t, B_o)$$

so if the decay terms are also included, the equations controlling the variation of the x, y and z components of the magnetisation with respect to time are given by:

$$\frac{d}{dt} M_x = -\gamma(- B_1 \sin\omega t\, M_z - B_o M_y) - M_x/T_2 \qquad 1\text{-}9a$$

$$\frac{d}{dt} M_y = -\gamma(B_o M_x - B_1 \cos\omega t\, M_z) - M_y/T_2 \qquad 1\text{-}9b$$

$$\frac{d}{dt} M_z = -\gamma(B_1 \cos\omega t\, M_y + B_1 \sin\omega t\, M_x) - (M_z - M_o)/T_1 \qquad 1\text{-}9c$$

These equations can be simplified by transferring to axes x^1, y^1, z which rotate at an angular frequency $-\omega$ in the xy plane. u, the component of $\underline{M}$ along x^1 and v, the component of $\underline{M}$ along y^1, can be related to the components of the magnetisation along the stationary axes thus:

$$u = M_x \cos(-\omega t) + M_y \sin(-\omega t) = M_x \cos\omega t - M_y \sin\omega t$$

$$v = -M_x \sin(-\omega t) + M_y \cos(-\omega t) = M_x \sin\omega t + M_y \cos\omega t$$

Equation 1-9 then becomes, in the new coordinate system (if $\gamma B_o = \omega_o$)

$$\frac{d}{dt} u = -(\omega - \omega_o) v - u/T_2 \qquad 1\text{-}10a$$

$$\frac{d}{dt} v = (\omega - \omega_o) u + B_1 M_z - v/T_2 \qquad 1\text{-}10b$$

$$\frac{d}{dt} M_z = -\gamma B_1 v - (M_z - M_o)/T_1 \qquad 1\text{-}10c$$

These are the Bloch equations[11,12].

The NMR spectrometer can be set up to observe either the in-phase component of the magnetisation, u (this is called the dispersion mode), or the out-of-phase component of the magnetisation, v (this is called the absorption mode).

1.2.2 Line Shapes and Saturation

For the usual continuous wave NMR experiment it can be assumed that to a close approximation

$$\frac{d}{dt} u = 0 \qquad \frac{d}{dt} v = 0 \qquad \frac{d}{dt} M_z = 0$$

With these conditions the Bloch equations can be solved to give the following expressions for u and v:

$$u = \gamma B_1 M_o T_2^2 (\omega_o - \omega) / [T_2^2 (\omega_o - \omega)^2 + \gamma^2 B_1^2 T_2 T_1 + 1] \qquad 1\text{-}11a$$

$$v = \gamma B_1 M_o T_2 / [T_2^2 (\omega_o - \omega)^2 + \gamma^2 B_1^2 T_2 T_1 + 1] \qquad 1\text{-}11b$$

$$M_z = M_o [T_2^2 (\omega_o - \omega)^2 + 1] / [T_2^2 (\omega_o - \omega)^2 + \gamma^2 B_1^2 T_2 T_1 + 1] \qquad 1\text{-}11c$$

The NMR experiment depends on the unequal populations of the two spin states available, the low energy state being more populated. For a thermally equilibrated Boltzmann distribution of nuclei in the two energy states:

$$N_2/N_1 = \exp(-\Delta U/k_B T)$$

where N_1 and N_2 are the populations of the low and high energy levels respectively

k_B is the Boltzmann constant

T is the absolute temperature

and ΔU is the energy level separation given by

$$\Delta U = 2\mu B_o$$

so $$N_2/N_1 = \exp(-2\mu B_o/k_B T) \qquad 1\text{-}12$$

and since $2\mu B_o/k_B T$ is small

$$N_2/N_1 = 1 - (2\mu B_o/k_B T)$$

The excess population in the lower state is

$$(N_1 - N_2)/N_1 = 2\mu B_o/k_B T$$

so when T = 291 K and B_o = 1 T then

$$(N_1 - N_2)/N_1 = 7 \times 10^{-6}$$

For every million nuclei in the lower energy level there are seven less nuclei in the upper energy level.

This excess population in the lower energy level absorbs energy from the radiofrequency field which excites some nuclei sufficiently to transfer them to the higher level. A strong radiofrequency field can

rapidly equalise the populations of the two levels thus reducing the height of the observed peak to zero. The reduction of the excess population by intense applied magnetic fields is called saturation and is one of the main operational problems in obtaining spectra suitable for lineshape analysis.

From the equation 1-12, the larger the magnetic field the greater is the excess population and the more widely spaced are the energy levels so, if the field is increased, saturation becomes less of a problem. The problem arises because the relaxation rate of nuclei is governed by the longitudinal relaxation time T_1 which may be of the order of 10^{-3} sec to 10 sec for liquids so, if the field B_1 is of sufficient intensity, the excess population of the lower level quickly reaches zero and the absorption signal is diminished or absent. In terms of the absorption line shape (equation 1-11) B_1 is sufficiently large that the term $\gamma^2 B_1^2 T_2 T_1$ is no longer much less than one so the height of the absorption peak decreases while the width of the peak increases[10].

1.2.3 Exchange Between Two Sites and the Absorption Lineshape

The equations for u and v (or for M_x and M_y) may be combined to give G, the complex magnetisation, which is defined as

$$G = u + iv \qquad 1\text{-}13a$$

Hence
$$\frac{d}{dt} G = \frac{d}{dt} u + i \frac{d}{dt} v \qquad 1\text{-}13b$$

Substituting from equation 1-10

$$\frac{d}{dt} G = -i(\omega_o - \omega)(u + iv) - (u + iv)/T_2 - i\omega_1 M_z$$

$$= -\alpha G + i \omega_1 M_z$$

where $\omega_1 = \gamma B_1$

and $\alpha = 1/T_2 + i(\omega_o - \omega)$.

Under steady state conditions $\frac{d}{dt} G = 0$

so $G = i\omega M_z/\alpha$ but since $M_z \simeq M_o$

$$G = i\omega M_o/\alpha$$

therefore $v = \mathcal{J}_m(G) = \omega_1 M_o T_2/(1 + T_2^2(\omega_o - \omega)^2)$

where $\mathcal{J}_m(G)$ is the imaginary part of G.

In a series of papers, Gutowsky and co-workers[9,13,14] and other groups[15,16] developed complete lineshape equations for the exchange of nuclei between two non-equivalent sites (with and without coupling) from the Bloch equations. The following treatment, however, is that of McConnell[17].

The jump of a nucleus from site A to site B and back again if τ_n (n = A, B) is the lifetime in site n and k_n the rate constant for exchange from site n, is equal to $1/\tau_n$ has the following effects on M, the magnetisation:

it decreases M at site A by $k_A G_A$

it increases M at site B by $k_A G_A$

it decreases M at site B by $k_B G_B$

it increases M at site A by $k_B G_B$

The magnetisation at sites A and B will therefore change according to equation 1-13B which, with the appropriate additional terms included gives the following equations:

$$\frac{d}{dt} G_A + \alpha_A G_A = i\omega_1 M_{zA} + k_B G_B - k_A G_A \qquad 1\text{-}14a$$

$$\frac{d}{dt} G_B + \alpha_B G_B = i\omega_1 M_{zB} + k_A G_A - k_B G_B \qquad 1\text{-}14b$$

Under steady state conditions

$$M_{zn} \simeq M_{on} = p_n M_o \quad \text{and} \quad \frac{d}{dt} G_n = 0 \quad \text{for} \quad n = A, B$$

If equations 1-14a and 1-14b are solved with the appropriate substitutions for M_{zn} then the total complex magnetisation G_T (defined as $G_A + B_B$) is given by the expression

$$G_T = \frac{i\omega_1 M_o \{\tau_A + \tau_B + \tau_A\tau_B(p_A\alpha_B + p_B\alpha_A)\}}{\{(\alpha_A\tau_A + 1)(\alpha_B\tau_B + 1) - 1\}} \qquad 1\text{-}15$$

where $$\alpha_n = + \frac{1}{T_{2n}} + i(\omega_o - \omega)$$

Since this exchange is between two sites the population at each site is related to the lifetime of the nuclei at that site of equilibrium:

i.e. $k_A p_A = k_B p_B$ or $p_A \tau_B = p_B \tau_A = \tau$ 1-16

Hence the absorption signal can be calculated from the imaginary parts of G according to the equation

$$v = \mathcal{J}_m(G) = \mathcal{J}_m \frac{i\omega_1 M_o\{\tau_A + \tau_B + \tau_A\tau_B(p_A\alpha_B + p_B\alpha_A)\}}{\{(\alpha_A\tau_A - 1)(\alpha_B\tau_B - 1) - 1\}} \qquad 1\text{-}17$$

if the quantities τ, p_A, p_B, T_{2A}, T_{2B}, ν_A, ν_B are given. It is also possible to specify set values for all parameters but τ and to vary τ by increments to obtain the closest possible match to an experimental spectrum. The quantities T_{2A}, T_{2B}, ν_A and ν_B are usually determined in the slow exchange limit when $\tau = \infty$.

This equation for the absorption lineshape has been derived by assuming that the signals in the low temperature limit are from a first order spectrum. If the spectrum is not first order then a density matrix approach should be used if a rigorous treatment is required[18].

1.2.4 Use of the Rate Constant

Once τ at each temperature is known then the Arrhenius equation can be used to find the activation energy E_a since

$$1/\tau = k = A \exp(-E_a/k_T) \qquad 1\text{-}18$$

where R is the gas constant

T is the absolute temperature

or the equation derived from transition state theory can be used.

$$1/\tau = k = k_B T/h \exp - (\Delta G^{\neq}/RT) \qquad 1\text{-}19$$

where k_B is the Boltzmann constant

T is the absolute temperature

h is Planck's constant

$\Delta G^{\neq}$ is the free energy difference of the transition state from the ground state

R is the gas constant

and $$\Delta G^{\neq} = \Delta H^{\neq} - T \Delta S^{\neq} \qquad 1\text{-}20$$

Since the full lineshape equation was very tedious to apply, the equation has at times been simplified to use such parameters as the intensity ratio of a maximum to the central minimum[19], the width of the peaks at half height both above[20] and below[21,22] the temperature at which the peaks coalesce, and the peak separation[14] to find a value for k at a specific temperature. The results obtained depended on the careful use of the simplified equations in the regions where the approximations made in their derivations are valid. If the equations were used outside this region the results were unreliable and led to discrepancies between the values quoted by different research groups.

By the time such disagreements in the magnitude of thermodynamic parameters had been well documented high speed computers were widely available so the full lineshape treatment could be used on systems such as the amides and selectively deuterated analogues which fulfilled the requirements of the Bloch lineshape equation that the spectrum in the slow exchange limit be first-order. As the number of total lineshape studies increased the agreement between the data from different research groups improved to the stage where external limitations on the accuracy of temperature, T_2 and position measurements were of greater importance in the determination of errors than the approximations used. Some approximations were made in cases such as formamide and acetamide[23] where coupling between the carbon-methyl group or proton and the nitrogen methyl groups could affect the relative intensity of the peaks, but in other cases such coupling is incorporated into the computer program[24].

The limitations of the absorption lineshape for two site exchange led to the generalization for first order exchange spectra of the Kubo Sack matrix approach[25] but for more complex spectra the most accurate possible description is given by the density matrix method[26,27]. At present lineshapes are analysed by the simplest possible method which will accurately describe the system so all three lineshape descriptions may be considered depending on the complexity of the spin system being studied.

1.2.5 Thermodynamic Parameters for Amide Systems

Many amides have been extensively studied by lineshape analysis in various solvents. In Table 1-1, data for N,N-dimethyl acetamide (DMA) has been collected from several papers which used complete lineshape analysis so the reported thermodynamic parameters should be accurate. The solvents used in these studies vary widely in polarity and reactivity (in the sense of associating with the solute) but unfortunately the parameters other than $\Delta G^{\neq}$ (the free energy of activation) vary, even for the same solvent, if analysed by different research groups.

When $\Delta G^{\neq}$ is considered the solvent has a marked effect on the magnitude of the free energy change. Changes in solvent alter the micro-environment of the solute so variations in $\Delta G^{\neq}$ with solvent can be expected. In the only study where the concentration of the DMA was varied purposefully on a large scale, $\Delta G^{\neq}$ does appear to change for the initial two dilutions but then seems to approach a limit. In this table, both deuterated and undeuterated DMA have been presented as though the thermodynamic parameters for rotation in these two compounds are the same. The data for DMA in formamide and neat DMA would seem to confirm this assumption; the discrepancies in thermodynamic parameters for DMA in D_2O and CCl_4 could be due to the differing concentrations of DMA used in these analyses and this would confirm the results for DMA

Table 1-1

N,N-Dimethylacetamide in Various Solvents

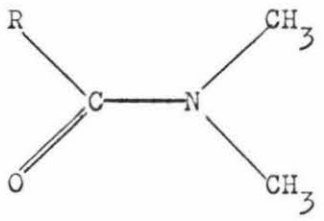

R	E_a[a] kJ mol^{-1}	$G^{\neq}_{298}$ kJ mol^{-1}	$S^{\neq}_{298}$ JK^{-1} mol^{-1}	Solvent	Conc.
CD_3[28]	82.0 ± 1.3	76.1	+ 11.3	neat	
CH_3[24]	79.5 ± 0.4	75.7 ± 0.4	+ 2.9 ± 4.1	neat	
CH_3[24]	82.8 ± 0.4	80.8 ± 0.4	+ 3.3 ± 4.1	D_2O	10 mol%
CD_3[23]	87.9 ± 3.8	80.8 ± 3.8	+ 11.3	D_2O	1.04M
CD_3[29]	84.9 ± 1.3	77.4	+ 17.2 ± 3.3	DMSO-d_6	9.5 mol%
CH_3[24]	82.0 ± 1.3	75.3	+ 13.0 ± 8.4	$(CD_3)_2CO$	10 mol%
CH_3[30]	70.5 ± 1.7	72.5	- 15.0 ± 5.1	CCl_4	14.9 mol%
CD_3[31]	76.6 ± 0.8	72.8	+ 4.6	CCl_4	1.7 mol%
CD_3[31]	75.3 ± 1.3	72.4	+ 2.1	Isooctane	2.6 mol%
CH_3[32]		77.4[b]		o-dichlorobenzene	20g l^{-1}
CD_3[33]	89.1 ± 2.5	81.2		Formamide	90.2 mol%
CH_3[33]	87.4 ± 1.7	80.8		Formamide	90.1 mol%
	82.0 ± 2.1	79.5			80.5 mol%
	81.6 ± 2.5	78.7			70.9 mol%
	81.6 ± 1.3	78.2			47.7 mol%

a $H^{\neq}_{298} = E_a - 2.5$ kJ mol^{-1}

b $G^{\neq}$ at 318K

in formamide.

Another way to change the environment of the solute is to use only one solvent but change its properties by adding salts of various kinds (Table 1-2). Very little work on this type of effect has been done so a coalescence temperature study by Egan[34] has been included. The two salt-free solutes at the head of the table are listed as controls on the reported parameters.

Temussi[23] attributes the large entropy change, $\Delta S^{\neq}$, for the DMA/Ag^{+}/D_2O solution to inaccurate T_2 values used to compensate for carbon-methyl coupling to the N-methyl groups. Such coupling was not explicitly included in the lineshape program but was treated as an extra broadening effect of the N-methyl peaks. To test whether $\Delta S^{\neq}$ was affected by T_2, analyses of N,N-dimethyltrideuteroacetamide in D_2O with and without the silver ion Ag^{+} were done at various temperatures. As the Table shows, attributing large values of $\Delta S^{\neq}$ to inaccurate T_2 values is probably correct for this molecule.

Unfortunately there are no systematic studies of salt effects on rotational barriers. The data in Table 1-2 show a marked change in $\Delta G^{\neq}_{298}$ in the presence of monovalent salts but more studies of ions in similar solvents are needed before theories about the interactions involved can be formulated.

Table 1-2

Salt Effects on Rotational Barriers in N,N-Dimethylacetamide

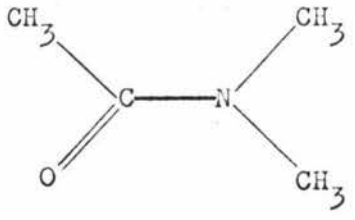

Ref	E_a kJ mol^{-1}	$G^{\neq}_{298}$ kJ mol^{-1}	$^{\neq}_{298}$ JK^{-1} mol^{-1}	Solvent
24	82.0 ± 1.3	75.3 ± 0.4	+ 13.0 ± 8.0	10 mol% $(CD_3)_3CO$
24	82.8 ± 1.3	80.6 ± 0.4	+ 3.3 ± 4.2	10 mol% D_2O
23	105.4 ± 2.1	74.1 ± 2.1	+ 85.4	1M D_2O + $4MAG^+$
23	79.5 ± 2.9	74.9 ± 2.9	± 5.9	1M DMA-d_3 in D_2O + $4MAG^+$
23	87.9 ± 3.8	80.8 ± 3.8	± 11.3	1M DMA-d_3 in D_2O
34		74.1[a]		1M dioxan
34		83.7[b]		1M dioxan + 1M Li^+

a $G^{\neq}$ at 333K

b $G^{\neq}$ at 374K